

# Switch-Based Iterative Learning Control for Tracking Iteration Varying References<sup>\*</sup>

Efe C. Balta<sup>\*</sup> Dawn M. Tilbury<sup>\*</sup> Kira Barton<sup>\*</sup>

<sup>\*</sup> *Department of Mechanical Engineering, University of Michigan, Ann Arbor, MI 48109, USA {baltaefe,tilbury,bartonk}@umich.edu*

---

**Abstract:** Iterative Learning Control (ILC) is a control strategy that improves the performance of repetitive systems by enabling near-perfect reference tracking. Iteration-invariant reference signals have been a fundamental assumption for most existing ILC developments. This assumption poses limitations on many applications of ILC where the iteration-varying reference is known to the controller a priori. This work presents a switch-based ILC scheme that combines the performance of standard ILC with guarantees on the error for switched reference signals. The proposed controller is formulated and its performance is analyzed. A simulation case study is provided at the end to illustrate the performance.

*Keywords:* Repetitive systems, iterative learning control (ILC), learning-based control

---

## 1. INTRODUCTION

Iterative Learning Control (ILC) is a control strategy that enables enhanced reference tracking in repetitive processes, where a reference signal is tracked by a dynamical process in each iteration. Repetitive processes often arise in industrial systems where a task is repeated in a cyclic manner, such as pick-and-place operations of a robot, or deposition of material by an additive manufacturing (AM) system on subsequent layers. Due to its wide application opportunities and its robustness to model uncertainty and disturbances, ILC has been extensively studied in the literature in both temporal (Barton and Alleyne, 2008; Ahn et al., 2007; Zsiga et al., 2016) and spatial domains (Hoelzle and Barton, 2016; Altin et al., 2018).

The repetitive process (the plant) considered in the ILC tracking problem is often a closed-loop system with a stabilizing feedback controller. Most of the classical results in ILC assume an iteration invariant reference, fixed iteration length, and fixed (and identical) initial conditions for each iteration. Typical ILC applications provide robustness with respect to iteration-invariant exogenous disturbances and model mismatch. Some important applications of ILC with repetitive processes include robotic precision motion stages (Altin and Barton, 2014; Barton and Alleyne, 2008), wafer scanning (Mishra et al., 2010), robotic pick-and-place operations (Freeman et al., 2010), and additive manufacturing (Hoelzle and Barton, 2016; Altin et al., 2018).

Some fundamental assumptions of ILC, such as iteration-invariant reference signals, limit the applicability of the approach for many practical implementations of interest. Developments in intelligent manufacturing systems allow for on-the-fly changes to the system references and tasks, which require control reconfiguration (Qamsane et al.,

2019). In this control reconfiguration scenario, the reference signal changes between iterations in a planned and predefined manner.

Another tracking problem of interest is in AM processes, where deposition in each layer is controlled by a feed-forward reference signal that prescribes the deposition path. After the material is deposited in a layer, the deposition system moves to the next layer to produce a 3D geometry in a layer-by-layer fashion. ILC has been used extensively in AM applications to track an iteration invariant deposition trajectory for each layer (Hoelzle et al., 2010; Altin et al., 2018). However, in practice, AM processes have multiple layers that have varying deposition paths (Balta et al., 2019; Guo and Mishra, 2016). Classical ILC developments fail to provide tracking performance guarantees under such iteration-varying references.

To compensate for iteration-varying references, multiple solutions have been proposed in the literature. In (Hoelzle et al., 2010) a method for partitioning common signals into individual bases and a framework for composing a reference for an iteration from these task-bases are proposed. The proposed controller achieves precise deposition tracking for a micro-AM application, but requires a training phase that may be impractical in a large-scale industrial setting. General methods for decomposing reference signals into polynomial and rational basis functions have also been proposed for iteration-varying references. An extensive framework for ILC with iteration-varying references is presented in (van Zundert et al., 2016) where rational basis functions are utilized in conjunction with online parameter identification techniques to provide a flexible ILC framework. Although an optimal performance with iteration-varying references is achieved, the performance is often conservative for the iterations with fixed reference when compared to standard ILC controllers. This is due to the fact that these developments aim to compensate for general iteration-varying references, which may result in conservative performance bounds. However, in many

---

<sup>\*</sup> This work was funded in part by NSF 1544678 and NIST Award No. 70NANB19H090.

practical applications as listed above, both the iteration at which a reference will switch and the new reference signal after the switch are known. In this work, we provide a novel switch-based ILC scheme that changes the learning law at the iteration of the known reference switch. The resulting ILC combines the tracking performance of standard ILC techniques and provides performance guarantees on the tracking error when the reference switches.

The contributions of this work are:

- Formulation of a novel switch-based ILC scheme for systems with known switched references
- Performance analysis and guarantees for the proposed controller for known switched references

The rest of the paper is structured as follows. Section 2 provides the notations, preliminaries on norm optimal ILC, and the problem formulation. Section 3 presents the proposed ILC scheme and provides a formal analysis of its performance. Section 4 provides a simulation case study to illustrate the performance of the proposed controller for various controller weights, references, and disturbances. Section 5 provides closing remarks and future directions.

## 2. PRELIMINARIES

### 2.1 Notation

$\mathbb{Z}^n$  and  $\mathbb{R}^n$  denote the set of  $n$ -dimensional integers and real numbers, respectively, and the subscripts  $+$  and  $+0$  denote the positive and nonnegative projections of these sets, respectively. Spectral radius of a matrix is denoted with  $\rho(\cdot)$ . The  $\ell_2$  norm of a vector  $\mathbf{x}$  and the corresponding induced norm of a matrix  $\mathbf{A}$  are denoted with  $\|\cdot\|$ . Additionally, the scaled, squared Euclidean-norm is denoted as  $\|\mathbf{x}\|_{\mathbf{W}}^2 = \mathbf{x}^T \mathbf{W} \mathbf{x}$ , for a symmetric positive definite matrix  $\mathbf{W}$ .

### 2.2 Norm-Optimal ILC

Norm-optimal ILC (NO-ILC) is a widely used control method in the literature (Ratcliffe et al., 2006; Barton and Alleyne, 2008; Hoelzle and Barton, 2016; Owens et al., 2012). Here we provide the preliminaries on the formulation of NO-ILC and some of its stability properties. Consider a discrete-time linear time-invariant (LTI) system with the dynamics given as:

$$\mathcal{H} : \begin{cases} x_k(t+1) &= \mathbf{A}x_k(t) + \mathbf{B}u_k(t) \\ y_k(t) &= \mathbf{C}x_k(t), \end{cases} \quad (1)$$

where  $t = 0, 1, \dots, (n_i - 1)$  is the discrete time index of length  $n_i \in \mathbb{Z}_+$  for an iteration,  $k = 1, 2, \dots$  is the iteration index,  $x_k(t) \in \mathbb{R}^{n_x}$ ,  $u_k(t) \in \mathbb{R}^{n_u}$ ,  $y_k(t) \in \mathbb{R}^{n_y}$  are the state vector, control input, and output of iteration  $k$ , respectively.  $\mathbf{A} \in \mathbb{R}^{n_x \times n_x}$ ,  $\mathbf{B} \in \mathbb{R}^{n_x \times n_u}$ , and  $\mathbf{C} \in \mathbb{R}^{n_y \times n_x}$  are the state, input, and output matrices. We assume that the pair  $(\mathbf{A}, \mathbf{B})$  is controllable and  $(\mathbf{A}, \mathbf{C})$  is observable. Next, we will denote the so-called ‘‘lifted’’ representation of (1) to evaluate the iteration dynamics of the system. Without loss of generality, we will assume an iteration invariant initial condition to be  $x_k(0) = 0$  for all  $k$ . Then, we have the iteration dynamics  $\mathbf{y}_k = \mathbf{H}\mathbf{u}_k$ , where  $k$  denotes the

iteration index,  $\mathbf{y}_k = [y_k(0)^T, y_k(1)^T, \dots, y_k(n_i - 1)^T]^T$ ,  $\mathbf{u}_k = [u_k(0)^T, u_k(1)^T, \dots, u_k(n_i - 1)^T]^T$ , and

$$\mathbf{H} = \begin{bmatrix} \mathbf{CB} & 0 & \dots & 0 \\ \mathbf{CAB} & \mathbf{CB} & \ddots & \vdots \\ \vdots & \vdots & \ddots & 0 \\ \mathbf{CA}^{n_i-1}\mathbf{B} & \mathbf{CA}^{n_i-2}\mathbf{B} & \dots & \mathbf{CB} \end{bmatrix}.$$

The iterative task for system (1) is for the output  $\mathbf{y}_k$  to track a repetitive reference  $\mathbf{r} \in \mathbb{R}^{n_i}$ . The reference  $\mathbf{r}$  is assumed to be the iteration-invariant and  $n_i$  dimensional discretized representation of a continuous reference signal. The control objective in NO-ILC is to follow the reference  $\mathbf{r}$  with minimum error with respect to the cost function

$$\mathcal{J} = \mathbf{e}_{k+1}^T \mathbf{Q} \mathbf{e}_{k+1} + \mathbf{u}_{k+1}^T \mathbf{S} \mathbf{u}_{k+1} + (\bar{\mathbf{u}}_{k+1})^T \mathbf{R} (\bar{\mathbf{u}}_{k+1}), \quad (2)$$

where  $\bar{\mathbf{u}}_{k+1} = \mathbf{u}_{k+1} - \mathbf{u}_k$ , the error for iteration  $k$  is given by  $\mathbf{e}_k = \mathbf{r} - \mathbf{y}_k$ , and  $(\mathbf{Q}, \mathbf{S}, \mathbf{R}) \triangleq (q\mathbf{I}, s\mathbf{I}, r\mathbf{I})$  are diagonal matrices with  $q, s, r \in \mathbb{R}_+$ . Minimizing  $\mathcal{J}$  with respect to  $\mathbf{u}_{k+1}$ , and rearranging the solution results in the NO-ILC update that has the form

$$\mathbf{u}_{k+1} = \mathbf{L}_u \mathbf{u}_k + \mathbf{L}_e \mathbf{e}_k, \quad (3a)$$

$$\mathbf{L}_u = (\mathbf{H}^T \mathbf{Q} \mathbf{H} + \mathbf{S} + \mathbf{R})^{-1} (\mathbf{H}^T \mathbf{Q} \mathbf{H} + \mathbf{R}), \quad (3b)$$

$$\mathbf{L}_e = (\mathbf{H}^T \mathbf{Q} \mathbf{H} + \mathbf{S} + \mathbf{R})^{-1} \mathbf{H}^T \mathbf{Q}, \quad (3c)$$

which results in the rearranged control input update given by  $\mathbf{u}_{k+1} = (\mathbf{L}_u - \mathbf{L}_e \mathbf{H}) \mathbf{u}_k + \mathbf{L}_e \mathbf{r}$ . Thus, the NO-ILC iteration scheme is asymptotically stable if  $\rho(\mathbf{L}_u - \mathbf{L}_e \mathbf{H}) \leq 1$ .

The control input reaches its steady state defined as  $\mathbf{u}_\infty \triangleq \lim_{k \rightarrow \infty} \mathbf{u}_k$  with the steady state error as  $\mathbf{e}_\infty = \mathbf{r} - \mathbf{H}\mathbf{u}_\infty$  and

the control  $\mathbf{u}_\infty = (\mathbf{I} - \mathbf{L}_u + \mathbf{L}_e \mathbf{H})^{-1} \mathbf{L}_e \mathbf{r}$  (Barton and Alleyne, 2008; Bristow, 2008). The convergence of NO-ILC is guaranteed by the asymptotic stability of the iterations, but it is often desirable to have monotonic convergence on the control signal to avoid large transients. The rate of convergence is given by  $\xi = \|\mathbf{L}_u - \mathbf{L}_e \mathbf{H}\|$ , for the convergent iterations  $\|\mathbf{u}_\infty - \mathbf{u}_{k+1}\| < \xi \|\mathbf{u}_\infty - \mathbf{u}_k\|$ , and a necessary condition for monotonic convergence is given as  $\xi < 1$ . In later discussions, this NO-ILC formulation is referred as the standard NO-ILC.

### 2.3 Problem Formulation

While the reference  $\mathbf{r}$  is assumed to be iteration-invariant in the classical NO-ILC developments, here we will analyze the problem where the input changes at a known iteration denoted as  $k'$ . Therefore, we have the following switching reference scheme:

$$\begin{cases} \mathbf{r} = \mathbf{r}_1 & \text{if } k < k' \\ \mathbf{r} = \mathbf{r}_2 & \text{if } k \geq k', \end{cases} \quad (4)$$

where  $\mathbf{r}_1, \mathbf{r}_2 \in \mathbb{R}^{n_i}$ . The control objective here is to minimize the error in each iteration and keep the error as close to zero as possible during the switch. In the context of this work, we name this problem as *the reference switching problem* and denote it with  $\mathcal{P}_s$ . Furthermore, we call the iteration at which the reference changes ( $k'$ ) a *switching iteration*. As mentioned before, we only consider  $\mathcal{P}_s$  for the cases where a switching iteration is known a priori to the controller.

The problem  $\mathcal{P}_s$  has practical applications in industry where the switching iteration  $k'$  and the switched refer-

ences  $\mathbf{r}_i$  are known a priori. Such applications include AM processes where cross-sectional geometry and the deposition path changes in predefined layers (Balta et al., 2019), pick-and-place robotic manipulators that switch their trajectory based on scheduled events (Qamsane et al., 2019), and reconfiguration of a milling process in which the cutting path is changed in a predefined manner.

Next, we provide a generalization and a standing assumption for the problem  $\mathcal{P}_s$  for completeness. The switching scheme in (4) is given for a switch between two references, but the reference switching problem generalizes to switching between  $n_s$  different references without loss of generality as long as the following assumption holds.

*Assumption 1.* The system (1) with the control input  $\mathbf{u}_k$  at iteration  $k = k' - 1$  is assumed to be in steady state so that we have  $\mathbf{u}_{k-1} = \mathbf{u}_k$  (i.e.  $\mathbf{u}_k = \mathbf{u}_\infty$ ) prior to the switching iteration  $k'$ .

This assumption holds well for monotonically convergent and exponentially convergent (Amann et al., 1996) NO-ILC. While this assumption may be stringent for certain systems, we utilize it in our preliminary work to provide performance guarantees. Thus, the error prior to the switching iteration is minimized and the controller converges to its steady-state  $\mathbf{u}_\infty$  in finite iterations. The rate of convergence is a design choice on the weights of the matrix  $\mathbf{R}$ , with  $\|\mathbf{R}\| = 0$  yielding immediate convergence and the rate approaching 0 as  $\|\mathbf{R}\| \rightarrow \infty$ . Here  $\|\mathbf{R}\| = \rho(\mathbf{R})$  since  $\mathbf{R} = r\mathbf{I}$  with  $r > 0$ .

While existing NO-ILC approaches provide perfect reference tracking and robust convergence guarantees for bounded disturbances, they do not provide guarantees on a bounded error when the reference of the system changes as given in (4). In this work, we will develop a switch-based NO-ILC scheme to provide guarantees and bounds on the  $\ell_2$  norm of the error in the switching iteration  $k'$ .

### 3. THE PROPOSED SWITCH-BASED NO-ILC

In this section, the proposed switch-based NO-ILC scheme and implementation of the proposed scheme for problem  $\mathcal{P}_s$  is presented and a performance analysis is given.

#### 3.1 Proposed Norm-Optimal Formulation

Here we derive a NO-ILC scheme for the known switching iteration  $k'$  according to (4) where the reference for the system switches from  $\mathbf{r}_1$  to  $\mathbf{r}_2$ . We assume that the switching iteration  $k'$  and the references  $\mathbf{r}_1, \mathbf{r}_2$  are known a priori and a NO-ILC controller for tracking  $\mathbf{r}_1$  is implemented for (1). We call this NO-ILC the *nominal* NO-ILC for the system in further discussion.

As stated before, the iteration error is given by  $\mathbf{e}_k = \mathbf{r} - \mathbf{H}\mathbf{u}_k$ . We have  $k = k' - 1$  with the reference as  $\mathbf{r} = \mathbf{r}_1$ , and  $k + 1 = k'$  with the reference  $\mathbf{r} = \mathbf{r}_2$ , as given in (4).

Based on Assumption 1, the system has a small error norm  $\|\mathbf{e}_k\| = \|\mathbf{e}_\infty\|$  at iteration  $k' - 1$ . Leveraging this fact, a switch-based NO-ILC at iteration  $k'$  minimizes the change in the error norm between iterations  $k' - 1$  and  $k'$  to keep the error norm small during the change of reference signal from  $\mathbf{r}_1$  to  $\mathbf{r}_2$ . The intuition behind this goal is to

utilize the controller for the already small tracking error of the system at iteration  $k' - 1$  to evaluate a control signal that will retain the small error at the switching iteration. Therefore, we have the two errors  $\mathbf{e}_k = \mathbf{r}_1 - \mathbf{H}\mathbf{u}_k$  and  $\mathbf{e}_{k+1} = \mathbf{r}_2 - \mathbf{H}\mathbf{u}_{k+1}$ . The proposed controller minimizes

$$\mathcal{J}_s = \bar{\mathbf{e}}_{k+1}^T \hat{\mathbf{Q}} \bar{\mathbf{e}}_{k+1} + \mathbf{u}_{k+1}^T \hat{\mathbf{S}} \mathbf{u}_{k+1} + (\bar{\mathbf{u}}_{k+1})^T \hat{\mathbf{R}} (\bar{\mathbf{u}}_{k+1}), \quad (5)$$

where,  $\bar{\mathbf{e}}_{k+1} = \mathbf{e}_{k+1} - \mathbf{e}_k$  denotes the difference of errors between consecutive iterations,  $(\hat{\mathbf{Q}}, \hat{\mathbf{S}}, \hat{\mathbf{R}}) \triangleq (\hat{q}\mathbf{I}, \hat{s}\mathbf{I}, \hat{r}\mathbf{I})$  are diagonal matrices with  $\hat{q}, \hat{s}, \hat{r} \in \mathbb{R}_+$ .

As with standard NO-ILC, we want to compute the control signal  $\mathbf{u}_{k+1}$  that minimizes the objective function  $\mathcal{J}_s$  in (5). Taking the partial derivative of  $\mathcal{J}_s$  with respect to  $\mathbf{u}_{k+1}$  yields

$\partial_{\mathbf{u}_{k+1}} \mathcal{J}_s = -\mathbf{H}^T \hat{\mathbf{Q}} (\bar{\mathbf{r}} - \mathbf{H}\bar{\mathbf{u}}_{k+1}) + (\hat{\mathbf{S}} + \hat{\mathbf{R}})\mathbf{u}_{k+1} - \hat{\mathbf{R}}\mathbf{u}_k$ , where,  $\bar{\mathbf{r}} = \mathbf{r}_2 - \mathbf{r}_1$ . Setting  $\partial_{\mathbf{u}_{k+1}} \mathcal{J}_s = 0$  and applying necessary substitutions, the resulting control update of the proposed switch-based NO-ILC is given by:

$$\hat{\mathbf{u}}_{k+1} = \hat{\mathbf{L}}_u \mathbf{u}_k + \hat{\mathbf{L}}_e (\mathbf{r}_2 - \mathbf{e}_k), \quad (6a)$$

$$\hat{\mathbf{L}}_u = \left( \mathbf{H}^T \hat{\mathbf{Q}} \mathbf{H} + \hat{\mathbf{S}} + \hat{\mathbf{R}} \right)^{-1} \hat{\mathbf{R}}, \quad (6b)$$

$$\hat{\mathbf{L}}_e = \left( \mathbf{H}^T \hat{\mathbf{Q}} \mathbf{H} + \hat{\mathbf{S}} + \hat{\mathbf{R}} \right)^{-1} \mathbf{H}^T \hat{\mathbf{Q}}. \quad (6c)$$

Note that by taking  $(\hat{\mathbf{Q}}, \hat{\mathbf{S}}, \hat{\mathbf{R}}) = (\mathbf{Q}, \mathbf{S}, \mathbf{R})$ , we have  $\hat{\mathbf{L}}_e = \mathbf{L}_e$ . The proposed switch-based NO-ILC utilizes the control  $\hat{\mathbf{u}}_{k+1}$  only for the trial  $k'$  where the reference switches. Since the objective of the controller is to minimize the change in error  $\ell_2$  norm between iterations, using the switch-based controller after the reference switches may result in an under-performing controller in the error norm between iterations. To avoid such responses and provide a controller with the performance of NO-ILC during the iterations with fixed reference, the following switching control scheme is provided for implementation.

- (1) Use NO-ILC with the choice of  $(\mathbf{Q}, \mathbf{S}, \mathbf{R})$  and the control iterations in (3) for iterations  $k = 1, \dots, k' - 1$
- (2) After iteration  $k' - 1$ , use (6) to evaluate the switching control with the choice of  $(\hat{\mathbf{Q}}, \hat{\mathbf{S}}, \hat{\mathbf{R}})$  and implement  $\hat{\mathbf{u}}_{k+1}$  for iteration  $k'$
- (3) After iteration  $k'$ , use the previous NO-ILC (although weights can be readjusted for the new reference) with the control iterations in (3) for future iterations ( $k \geq k' + 1$ ).

#### 3.2 Performance Analysis

The main theorem to guarantee the tracking performance of the proposed switch-based controller for problem  $\mathcal{P}_s$  is presented next.

*Theorem 2.* For problem  $\mathcal{P}_s$ , the switch-based NO-ILC in (6) with the weights  $(\hat{\mathbf{Q}}, \hat{\mathbf{S}}, \hat{\mathbf{R}}) = (\mathbf{Q}, \mathbf{S}, \mathbf{R})$  and control input  $\hat{\mathbf{u}}_{k'}$  is guaranteed to yield a better performance in the sense that we get  $d = \|\boldsymbol{\eta}_2\|^2 - \|\boldsymbol{\eta}_1\|^2 < 0$ , where,  $\boldsymbol{\eta}_1 = \mathbf{r}_2 - \mathbf{H}\mathbf{u}_{k'}$  and  $\boldsymbol{\eta}_2 = \mathbf{r}_2 - \mathbf{H}\hat{\mathbf{u}}_{k'}$  at the switching iteration  $k'$  if we have  $(\bar{\mathbf{r}} - \mathbf{e}_k)^T (\boldsymbol{\Gamma}^T \boldsymbol{\Gamma} - 2\boldsymbol{\Gamma}) (\bar{\mathbf{r}} - \mathbf{e}_k) < 4\mathbf{e}_k^T \boldsymbol{\Gamma} (\bar{\mathbf{r}} - \mathbf{e}_k)$ , where  $k = k' - 1$ ,  $\bar{\mathbf{r}} = \mathbf{r}_2 - \mathbf{r}_1$ , and  $\boldsymbol{\Gamma} = \mathbf{H}\hat{\mathbf{L}}_e$ .

**Proof.** First we want to analyze if the proposed iteration in (6) with  $\hat{\mathbf{u}}_{k+1}$  yields a smaller error norm when compared to the nominal NO-ILC with the input  $\mathbf{u}_{k+1}$

evaluated according to (3) for the switching iteration  $k'$ . For this purpose, we consider two errors  $\boldsymbol{\eta}_1 = \mathbf{r}_2 - \mathbf{H}\mathbf{u}_{k+1}$  and  $\boldsymbol{\eta}_2 = \mathbf{r}_2 - \mathbf{H}\hat{\mathbf{u}}_{k+1}$  and analyze the sign of the following difference of error norms  $d = \|\boldsymbol{\eta}_2\|^2 - \|\boldsymbol{\eta}_1\|^2$ , noting that  $k = k' - 1$ . We expand this difference in the following

$$\begin{aligned} d &= \hat{\mathbf{u}}_{k+1}^T \mathbf{H}^T \mathbf{H} \hat{\mathbf{u}}_{k+1} - \mathbf{u}_{k+1}^T \mathbf{H}^T \mathbf{H} \mathbf{u}_{k+1} - 2\mathbf{r}_2^T \mathbf{H} \tilde{\mathbf{u}}_{k+1}, \\ &= (\hat{\mathbf{u}}_{k+1} + \mathbf{u}_{k+1})^T \mathbf{H}^T \mathbf{H} \tilde{\mathbf{u}}_{k+1} - 2\mathbf{r}_2^T \mathbf{H} \tilde{\mathbf{u}}_{k+1}, \\ &= \tilde{\mathbf{u}}_{k+1}^T \mathbf{H}^T \mathbf{H} \tilde{\mathbf{u}}_{k+1} - 2\boldsymbol{\eta}_1^T \mathbf{H} \tilde{\mathbf{u}}_{k+1}, \end{aligned} \quad (7)$$

where  $\tilde{\mathbf{u}}_{k+1} = \hat{\mathbf{u}}_{k+1} - \mathbf{u}_{k+1}$ . Additionally, rearranging (6) we have

$$\hat{\mathbf{u}}_{k+1} = \mathbf{M}^{-1}(\mathbf{R} + \mathbf{H}^T \mathbf{Q} \mathbf{H}) \mathbf{u}_k + \mathbf{M}^{-1} \mathbf{H}^T \mathbf{Q} \tilde{\mathbf{r}},$$

where  $\mathbf{M} = \mathbf{H}^T \hat{\mathbf{Q}} \mathbf{H} + \hat{\mathbf{S}} + \hat{\mathbf{R}}$ . Here, let  $(\hat{\mathbf{Q}}, \hat{\mathbf{S}}, \hat{\mathbf{R}}) = (\mathbf{Q}, \mathbf{S}, \mathbf{R})$  without loss of generality. Then, it can be shown that we have  $\hat{\mathbf{u}}_{k+1} = \mathbf{L}_u \mathbf{u}_k + \mathbf{L}_e \tilde{\mathbf{r}}$  and we get  $\tilde{\mathbf{u}}_{k+1} = \mathbf{L}_e (\tilde{\mathbf{r}} - \mathbf{e}_k)$ . Additionally, using Assumption 1 we have  $\mathbf{u}_k = \mathbf{u}_{k-1}$  thus,  $\boldsymbol{\eta}_1 = \mathbf{r}_2 - \mathbf{H}\mathbf{u}_{k+1} = \mathbf{r}_2 - \mathbf{H}\mathbf{u}_k = \tilde{\mathbf{r}} + \mathbf{e}_k$ . Then (7) becomes

$$\begin{aligned} d &= (\tilde{\mathbf{r}} - \mathbf{e}_k)^T \mathbf{L}_e^T \mathbf{H}^T \mathbf{H} \mathbf{L}_e (\tilde{\mathbf{r}} - \mathbf{e}_k) \\ &\quad - 2(\tilde{\mathbf{r}} + \mathbf{e}_k)^T \mathbf{H} \mathbf{L}_e (\tilde{\mathbf{r}} - \mathbf{e}_k), \\ &= (\tilde{\mathbf{r}} - \mathbf{e}_k)^T (\boldsymbol{\Gamma}^T \boldsymbol{\Gamma} - 2\boldsymbol{\Gamma}) (\tilde{\mathbf{r}} - \mathbf{e}_k) - 4\mathbf{e}_k^T \boldsymbol{\Gamma} (\tilde{\mathbf{r}} - \mathbf{e}_k), \end{aligned}$$

where  $\boldsymbol{\Gamma} = \mathbf{H} \mathbf{L}_e$ . The following necessary and sufficient condition guarantees  $d \leq 0$ , which implies that the error norm of the proposed controller is at most the same as the error norm of the nominal controller, given as:

$$(\tilde{\mathbf{r}} - \mathbf{e}_k)^T (\boldsymbol{\Gamma}^T \boldsymbol{\Gamma} - 2\boldsymbol{\Gamma}) (\tilde{\mathbf{r}} - \mathbf{e}_k) \leq 4\mathbf{e}_k^T \boldsymbol{\Gamma} (\tilde{\mathbf{r}} - \mathbf{e}_k),$$

which completes the proof.  $\square$

Theorem 2 provides necessary and sufficient conditions for the proposed switching controller to not under-perform when compared to a nominal NO-ILC. Note that the analysis is provided for the case when  $(\hat{\mathbf{Q}}, \hat{\mathbf{S}}, \hat{\mathbf{R}}) = (\mathbf{Q}, \mathbf{S}, \mathbf{R})$ , but it can be extended to the cases where the weights are different between the nominal and switch-based NO-ILC.

A performance analysis for the conditions under which we get  $d < 0$  (see Theorem 2) is given next. Due to Assumption 1, we can further conclude that we have  $\|\mathbf{e}_k\| = \|\mathbf{e}_\infty\| < \epsilon$  at the iteration  $k = k' - 1$  where,  $\epsilon > 0$  is a small number that can be estimated based on the NO-ILC design. Thus, we assume that  $\|\mathbf{e}_{k'-1}\| < \epsilon < \|\tilde{\mathbf{r}}\|$  holds in general for a (scaled) Euclidean norm.

*Corollary 3.* If the matrix  $\boldsymbol{\Gamma} = \mathbf{H} \mathbf{L}_e$  is symmetric positive definite with  $\rho(\boldsymbol{\Gamma}) < 1$ , and if we have  $3\|\mathbf{e}_{k'-1}\|_{\boldsymbol{\Gamma}} < \|\tilde{\mathbf{r}}\|_{\boldsymbol{\Gamma}}$ , then the Theorem 2 holds, i.e. we get  $d = \|\boldsymbol{\eta}_2\|^2 - \|\boldsymbol{\eta}_1\|^2 < 0$ , where  $\boldsymbol{\eta}_1 = \mathbf{r}_2 - \mathbf{H}\mathbf{u}_{k+1}$  and  $\boldsymbol{\eta}_2 = \mathbf{r}_2 - \mathbf{H}\hat{\mathbf{u}}_{k+1}$ .

**Proof.** First, note that for a symmetric positive definite matrix  $\mathbf{P} \in \mathbb{R}^{n \times n}$  with  $\rho(\mathbf{P}) < 1$  we have  $\mathbf{x}^T \mathbf{P}^T \mathbf{P} \mathbf{x} < \mathbf{x}^T \mathbf{P} \mathbf{x}$ ,  $\mathbf{x} \in \mathbb{R}^n$ . Then the following holds for some  $\gamma > 0$ :

$$\|\tilde{\mathbf{r}} - \mathbf{e}_k\|_{\boldsymbol{\Gamma}^T \boldsymbol{\Gamma}}^2 - \|\tilde{\mathbf{r}} - \mathbf{e}_k\|_{\boldsymbol{\Gamma}}^2 < \gamma \|\tilde{\mathbf{r}} - \mathbf{e}_k\|_{\boldsymbol{\Gamma}}, \quad (8)$$

where  $k = k' - 1$ , which holds with strict inequality since the left-hand side is a negative number (due to  $\rho(\boldsymbol{\Gamma}) < 1$ ) while the right-hand side is positive. Then, noting  $\|\tilde{\mathbf{r}}\|_{\boldsymbol{\Gamma}} - 3\|\mathbf{e}_k\|_{\boldsymbol{\Gamma}} > 0$ , the following holds:

$$\begin{aligned} \|\tilde{\mathbf{r}}\|_{\boldsymbol{\Gamma}} - 3\|\mathbf{e}_k\|_{\boldsymbol{\Gamma}} &= 2(\|\tilde{\mathbf{r}}\|_{\boldsymbol{\Gamma}} - \|\mathbf{e}_k\|_{\boldsymbol{\Gamma}}) - (\|\tilde{\mathbf{r}}\|_{\boldsymbol{\Gamma}} + \|\mathbf{e}_k\|_{\boldsymbol{\Gamma}}), \\ &\leq 2(\|\tilde{\mathbf{r}}\|_{\boldsymbol{\Gamma}} - \|\mathbf{e}_k\|_{\boldsymbol{\Gamma}}) - \|\tilde{\mathbf{r}} - \mathbf{e}_k\|_{\boldsymbol{\Gamma}}, \end{aligned} \quad (9)$$

where we use the fact  $\|\mathbf{x}\| + \|\mathbf{y}\| \geq \|\mathbf{x} - \mathbf{y}\|$ ,  $\mathbf{x}, \mathbf{y} \in \mathbb{R}^n$ . Now, let  $\gamma = 2(\|\tilde{\mathbf{r}}\|_{\boldsymbol{\Gamma}} - \|\mathbf{e}_k\|_{\boldsymbol{\Gamma}}) - \|\tilde{\mathbf{r}} - \mathbf{e}_k\|_{\boldsymbol{\Gamma}}$ , where clearly  $\gamma > 0$  (due to (9)), and re-arrange (8) as:

$$\begin{aligned} \|\tilde{\mathbf{r}} - \mathbf{e}_k\|_{\boldsymbol{\Gamma}^T \boldsymbol{\Gamma}}^2 &< (\|\tilde{\mathbf{r}} - \mathbf{e}_k\|_{\boldsymbol{\Gamma}} + \gamma) \|\tilde{\mathbf{r}} - \mathbf{e}_k\|_{\boldsymbol{\Gamma}}, \\ &= 2(\|\tilde{\mathbf{r}}\|_{\boldsymbol{\Gamma}} - \|\mathbf{e}_k\|_{\boldsymbol{\Gamma}}) \|\tilde{\mathbf{r}} - \mathbf{e}_k\|_{\boldsymbol{\Gamma}}, \\ &\leq 2((\|\tilde{\mathbf{r}}\|_{\boldsymbol{\Gamma}} - \|\mathbf{e}_k\|_{\boldsymbol{\Gamma}}) (\|\tilde{\mathbf{r}}\|_{\boldsymbol{\Gamma}} + \|\mathbf{e}_k\|_{\boldsymbol{\Gamma}})), \\ &= 2(\|\tilde{\mathbf{r}}\|_{\boldsymbol{\Gamma}}^2 - \|\mathbf{e}_k\|_{\boldsymbol{\Gamma}}^2), \\ &= 2(\tilde{\mathbf{r}} + \mathbf{e}_k)^T \boldsymbol{\Gamma} (\tilde{\mathbf{r}} - \mathbf{e}_k), \\ &= 4\mathbf{e}_k^T \boldsymbol{\Gamma} (\tilde{\mathbf{r}} - \mathbf{e}_k) + (\tilde{\mathbf{r}} - \mathbf{e}_k)^T 2\boldsymbol{\Gamma} (\tilde{\mathbf{r}} - \mathbf{e}_k), \end{aligned} \quad (10)$$

where we again use the fact  $\|\mathbf{x}\| + \|\mathbf{y}\| \geq \|\mathbf{x} - \mathbf{y}\|$ ,  $\mathbf{x}, \mathbf{y} \in \mathbb{R}^n$  and the identity  $a^2 - b^2 = (a - b)(a + b)$ ,  $a, b \in \mathbb{R}$ . The expression (10) can be rewritten as  $(\tilde{\mathbf{r}} - \mathbf{e}_k)^T (\boldsymbol{\Gamma}^T \boldsymbol{\Gamma} - 2\boldsymbol{\Gamma}) (\tilde{\mathbf{r}} - \mathbf{e}_k) < 4\mathbf{e}_k^T \boldsymbol{\Gamma} (\tilde{\mathbf{r}} - \mathbf{e}_k)$ , which implies that we have  $d < 0$  by Theorem 2 and concludes the proof.  $\square$

To see when  $\boldsymbol{\Gamma}$  is symmetric positive definite, note that  $\boldsymbol{\Gamma} = \mathbf{H} \mathbf{M}^{-1} \mathbf{H}^T \hat{\mathbf{Q}}$ , with  $\mathbf{M} = \mathbf{H}^T \hat{\mathbf{Q}} \mathbf{H} + \hat{\mathbf{S}} + \hat{\mathbf{R}}$ . Since  $\mathbf{M}$  is positive definite (by the fact that  $\hat{q}, \hat{s}, \hat{r} \in \mathbb{R}_+$ ), we denote its singular value decomposition (SVD) as  $\mathbf{M} = \mathbf{D} \mathbf{V} \mathbf{D}^T$ , where  $\mathbf{V} = \hat{q} \mathbf{V}_2 + \hat{\mathbf{S}} + \hat{\mathbf{R}}$  and we have the SVD  $\mathbf{H}^T \mathbf{H} = \mathbf{D} \mathbf{V}_2 \mathbf{D}^T$ , where we assume  $\mathbf{H}$  is full rank without loss of generality. Therefore, by noting that  $\hat{\mathbf{Q}} = \hat{q} \mathbf{I}$ , we have  $\boldsymbol{\Gamma} = \mathbf{H} \mathbf{D} \hat{q} \mathbf{V}^{-1} \mathbf{D}^T \mathbf{H}^T \succ 0$ .

#### 4. SIMULATION CASE STUDY

Illustration of the proposed controller on a simple double integrator is given in this section. The proposed switch-based NO-ILC controller is compared to a nominal NO-ILC scheme with different weights.

##### 4.1 Simulation Setup

A damped rigid body system dynamics with a time discretization of 0.025 seconds is used in the case study. The discrete-time LTI dynamics of the system are given in the following.

$$\begin{aligned} \mathbf{x}_k(t+1) &= \begin{bmatrix} 0.9997 & 0.0248 \\ -0.0248 & 0.9873 \end{bmatrix} \mathbf{x}_k(t) + \begin{bmatrix} 0.0003 \\ 0.0248 \end{bmatrix} \mathbf{u}_k(t), \\ \mathbf{y}_k(t) &= [1 \quad 0] \mathbf{x}_k(t). \end{aligned}$$

We have iteration length as  $\tau \in [0, 10]$  seconds and the time is discretized in 0.05 second intervals so that the discrete time index for an iteration has  $n_i = 201$  (e.g.  $t = 0, 1, \dots, 200$ ). References  $r_1(t) = \sin(0.05t)$  and  $r_2(t) = \sin(0.0375t)$  are defined as the two references for the system to track, and the corresponding time-discretized reference vectors  $\mathbf{r}_1, \mathbf{r}_2 \in \mathbb{R}^{n_i}$  are computed accordingly. The initial condition is given as  $\mathbf{x}_k(0) = 0$  for all  $k$ . 20 iterations are performed for each simulation study and the reference is switched according to

$$\begin{cases} \mathbf{r} = \mathbf{r}_1 & \text{if } k < 11 \\ \mathbf{r} = \mathbf{r}_2 & \text{if } k \geq 11. \end{cases} \quad (11)$$

The two references used in the case study are shown in Fig. 1. Therefore, the system output  $\mathbf{y}_k$  should track reference  $\mathbf{r}_1$  during iterations  $k \in [1, 10]$ , and reference  $\mathbf{r}_2$  during iterations  $k \in [11, 20]$ .

The proposed switch-based NO-ILC scheme is implemented in the simulation so that for iterations  $k \in [1, 10]$  the nominal NO-ILC is used. The proposed ILC in (6) is used for the switching iteration  $k' = 11$ . The nominal NO-ILC is used for the remaining iterations  $k \in [12, 20]$ . The

weights of the nominal NO-ILC are kept constant prior to and after the switching iteration for all simulations.

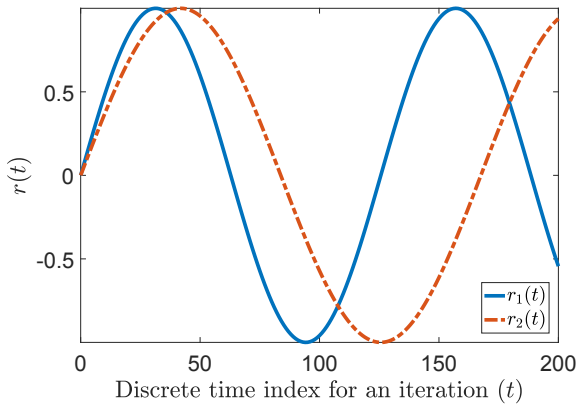


Fig. 1. References used in the case study with  $r_1(t) = \sin(0.05t)$  for  $k \in [1, 10]$  and  $r_2(t) = \sin(0.0375t)$  for  $k \in [11, 20]$ .

Three different weights for the nominal NO-ILC are provided in Table 1. Nominal NO-ILC 1 is the aggressive setting, nominal NO-ILC 2 has a higher  $\mathbf{R}$  for high measurement noise, and nominal NO-ILC 3 is robust to the changes in reference with  $\mathbf{S}$ . The switch-based NO-ILC weights are set equal to the corresponding nominal NO-ILC. Two sets of simulation results are shown. The noise-free simulation case is when we assume that the output  $y_k(t)$  is measured without any noise.

Table 1. Simulation setup weights

| Design           | Parameters   |
|------------------|--|
| Nominal NO-ILC 1 | $\mathbf{Q} = 10^2 \mathbf{I}, \mathbf{S} = 10^{-4} \mathbf{I}, \mathbf{R} = 10^{-5} \mathbf{I}$                   |
| Nominal NO-ILC 2 | $\mathbf{Q} = 10^2 \mathbf{I}, \mathbf{S} = 10^{-4} \mathbf{I}, \mathbf{R} = 10^{-2} \mathbf{I}$                   |
| Nominal NO-ILC 3 | $\mathbf{Q} = 10^2 \mathbf{I}, \mathbf{S} = 10^{-2} \mathbf{I}, \mathbf{R} = 10^{-5} \mathbf{I}$                   |
| (C1)             | $\hat{\mathbf{Q}} = 10^2 \mathbf{I}, \hat{\mathbf{S}} = 10^{-4} \mathbf{I}, \hat{\mathbf{R}} = 10^{-5} \mathbf{I}$ |
| (C2)             | $\hat{\mathbf{Q}} = 10^2 \mathbf{I}, \hat{\mathbf{S}} = 10^{-4} \mathbf{I}, \hat{\mathbf{R}} = 10^{-2} \mathbf{I}$ |
| (C3)             | $\hat{\mathbf{Q}} = 10^2 \mathbf{I}, \hat{\mathbf{S}} = 10^{-2} \mathbf{I}, \hat{\mathbf{R}} = 10^{-5} \mathbf{I}$ |

For the simulation with noise, a multivariate normal noise with zero mean and a covariance matrix given by  $\Sigma = 0.056^2 \mathbf{I}$  is applied to the system. The random variable has the distribution  $\nu_k \sim \mathcal{N}(\mathbf{0}, \Sigma)$  and is added to the measurements so we have  $\mathbf{y}_k = \mathbf{H}\mathbf{u}_k + \nu_k$ . The mean and covariance of the noise  $\nu_k$  are kept constant in each iteration but a new random vector is sampled from the distribution for each iteration  $k$  (i.e. i.i.d. samples). All the controllers are initiated with  $u_1(t) = 0$  for the first iteration  $k = 1$  so that the controller learns from the response of the system with zero input, which is a standard practice with most ILC applications in literature.

#### 4.2 Results and Discussion

Figure 2 shows the simulation results for the noise-free measurement case. In all results, the vertical axes show the ratio of error norm of an iteration  $\|e_k\|$  to the error norm for the first iteration  $\|e_1\|$  on a logarithmic scale.

Table 2. Simulation results for RMS of  $\|e_k\|$

| Design | RMS (noise-free) | RMS (with noise) |
|--------|------------------|------------------|
| (C1)   | 2.1862           | 2.1890           |
| (C2)   | 2.1869           | 2.1896           |
| (C3)   | 2.1910           | 2.1930           |

The nominal NO-ILCs track the initial reference  $r_1$  well until the switching iteration. At the switching iteration, the nominal NO-ILC controller expects the reference  $r_1$ , but the reference is now switched to  $r_2$ . Due to the reference switch, the error norm spikes to a level even higher than the initial error norm with  $u_1(t) = 0$ . The spike is highest for the aggressive controller in nominal NO-ILC 1, and it is the lowest among the nominal NO-ILCs for nominal NO-ILC-3, which is an expected result by design. After the switching iteration, the nominal NO-ILC tracks the new reference  $r_2$ . Note that since the rate of change in the second reference  $r_2$  is less than  $r_1$ , the nominal NO-ILC yields a better tracking performance with the switched reference. This behavior is observed in all simulations.

The proposed switch-based NO-ILC controller with three different sets of weights ((C1), (C2), (C3)) yields a better performance on the switching iteration when compared to nominal NO-ILC as shown in Fig. 2. The root mean squares of the error norms are in Table 2. Therefore we confirm that the more aggressive tuning in (C1) outperforms the conservative tunings for the noise-free simulation.

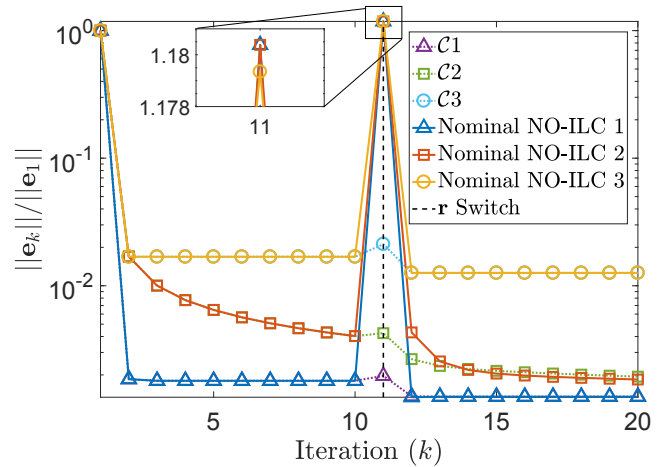


Fig. 2. Results of the case study for the noise-free measurements. The switching iteration  $k' = 11$  is shown with a dashed black vertical line.

Figure 3 shows the simulation results where the output has the noise given by  $\nu_k$ . Due to the noise in measurements, we see that the performance of all the controllers are worse than the ones shown in the noise-free simulations. In the noisy setting, the spike is again the highest for the aggressive controller in nominal NO-ILC 1, and it is the lowest among the nominal NO-ILCs for nominal NO-ILC 2 as expected by its design. The root mean squares of the error norms are shown in Table 2. Therefore we see that utilizing a more conservative set of gains in (C2) does not yield a performance improvement with the switch-based NO-ILC, and it provides a worse convergence performance

when compared to (C1). Similarly, the robust nominal NO-ILC 3 and the corresponding controller (C3) yields a worse performance with a higher error when compared to the aggressive gain setting on (C1). Thus, we conclude that the choice of aggressive tunings for the proposed controller yields a more desirable performance and should be favored for the case of switching references.

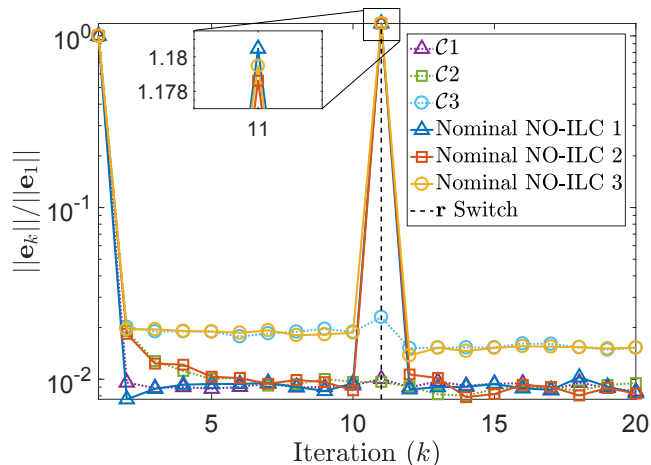


Fig. 3. Results of the case study for the noisy measurements. The switching iteration  $k' = 11$  is shown with a dashed black vertical line.

The results show that in both noisy and noise-free simulations, the proposed switched controller works well and guarantees bounded error norm at the switching iteration as given by Theorem 2 and Corollary 3. Since the controller has a switched structure with a nominal ILC for the iterations other than the switching iteration, it can be combined with many of the existing ILC schemes.

## 5. CONCLUSION AND FUTURE WORK

In this paper, a novel switched ILC scheme is presented for systems with known iteration-varying (switched) references. The proposed controller provides guarantees on the error norm at the switching iteration. Additionally, the switching controller implementation scheme provides a flexible framework to integrate the proposed controller with existing ILC techniques.

Future work will look into analyzing the proposed controller under measurement and input noises in the process as well as modeling uncertainties. Additionally, relaxing the steady-state nominal ILC assumption to consider cases where the controlled system is in its transient response in the iteration domain is of interest.

## REFERENCES

Ahn, H.S., Moore, K.L., and Chen, Y. (2007). Stability analysis of discrete-time iterative learning control systems with interval uncertainty. *Automatica*, 43(5), 892–902.

Altin, B. and Barton, K. (2014). Robust iterative learning for high precision motion control through L1 adaptive feedback. *Mechatronics*, 24(6), 549–561.

Altin, B., Wang, Z., Hoelzle, D.J., and Barton, K. (2018). Robust monotonically convergent spatial iterative learning control: Interval systems analysis via discrete fourier

transform. *IEEE Transactions on Control Systems Technology*.

Amann, N., Owens, D.H., and Rogers, E. (1996). Iterative learning control for discrete-time systems with exponential rate of convergence. *IEE Proceedings-Control Theory and Applications*, 143(2), 217–224.

Balta, E.C., Tilbury, D.M., and Barton, K. (2019). Control-oriented modeling and layer-to-layer stability for fused deposition modeling: a kernel basis approach. In *2019 American Control Conference (ACC)*, 4727–4733. IEEE.

Barton, K.L. and Alleyne, A.G. (2008). A cross-coupled iterative learning control design for precision motion control. *IEEE Transactions on Control Systems Technology*, 16(6), 1218–1231.

Bristow, D.A. (2008). Weighting matrix design for robust monotonic convergence in norm optimal iterative learning control. In *2008 American Control Conference*, 4554–4560. IEEE.

Freeman, C.T., Lewin, P.L., Rogers, E., and Ratcliffe, J.D. (2010). Iterative learning control applied to a gantry robot and conveyor system. *Transactions of the Institute of Measurement and Control*, 32(3), 251–264.

Guo, Y. and Mishra, S. (2016). A predictive control algorithm for layer-to-layer ink-jet 3D printing. In *2016 American Control Conference (ACC)*, 833–838. IEEE.

Hoelzle, D.J., Alleyne, A.G., and Johnson, A.J.W. (2010). Basis task approach to iterative learning control with applications to micro-robotic deposition. *IEEE Transactions on Control Systems Technology*, 19(5), 1138–1148.

Hoelzle, D.J. and Barton, K.L. (2016). On spatial iterative learning control via 2-D convolution: Stability analysis and computational efficiency. *IEEE Transactions on Control Systems Technology*, 24(4), 1504–1512.

Mishra, S., Topcu, U., and Tomizuka, M. (2010). Optimization-based constrained iterative learning control. *IEEE Transactions on Control Systems Technology*, 19(6), 1613–1621.

Owens, D.H., Freeman, C.T., and Van Dinh, T. (2012). Norm-optimal iterative learning control with intermediate point weighting: theory, algorithms, and experimental evaluation. *IEEE Transactions on Control Systems Technology*, 21(3), 999–1007.

Qamsane, Y., Balta, E.C., Moyne, J., Tilbury, D., and Barton, K. (2019). Dynamic rerouting of cyber-physical production systems in response to disruptions based on SDC framework. In *2019 American Control Conference (ACC)*, 3650–3657. IEEE.

Ratcliffe, J.D., Lewin, P.L., Rogers, E., Htnen, J.J., and Owens, D.H. (2006). Norm-optimal iterative learning control applied to gantry robots for automation applications. *IEEE Transactions on Robotics*, 22(6), 1303–1307.

van Zundert, J., Bolder, J., and Oomen, T. (2016). Optimality and flexibility in iterative learning control for varying tasks. *Automatica*, 67, 295–302.

Zsiga, N., van Dooren, S., Elbert, P., and Onder, C.H. (2016). A new method for analysis and design of iterative learning control algorithms in the time-domain. *Control Engineering Practice*, 57, 39–49.